

# Journal of Molecular Science

## Formulation And Characterization Of Diosgenin Proniosomes For Improved Skin Permeation

Mr. Jeevan Bholenath Kore<sup>1</sup>, Dr. Harshada A. Patil\*<sup>2</sup>, Ms. Shraddha Sanjay Kothale<sup>3</sup>, Mrs. Ashwini Appaso Todkar<sup>4</sup>, Mr. Mahesh Tanaji Kore<sup>5</sup>

<sup>1</sup>Research Scholar, Department of Pharmaceutical Chemistry, Appasaheb Birnale college of Pharmacy, Sangli. 414416

<sup>2</sup>Associate Professor, Department of Pharmaceutics, Bharati Vidyapeeth college of Pharmacy, Palus. 416310

<sup>3</sup>Research Scholar, Department of Pharmacology, Dr. Shivajirao Kadam college of Pharmacy, Kasbe Digras, Sangli. 416305

<sup>4</sup>Assistant Professor, Department of Pharmaceutics, Sharad Pharmacy institute Yadrav, Ichalkaranji. 416115

<sup>5</sup>Research Scholar, Department of Pharmaceutics, Annasaheb Dange College of B. Pharmacy, Ashta. 416301

### Article Information

Received: 27-10-2025

Revised: 14-11-2025

Accepted: 24-11-2025

Published: 22-12-2025

### Keywords

*Diosgenin, Proniosomes, Transdermal delivery, Span 60, Skin permeation, Cosmeceutical formulation, Vesicular drug delivery system, Coacervation phase separation.*

### ABSTRACT

The goal of the current study was to improve the topical penetration and delivery performance of diosgenin by creating and assessing a proniosomal formulation. Using Span 60 and cholesterol, the coacervation phase separation method was used to create diosgenin-loaded proniosomes, which were then optimized among seven formulations. With a mean vesicle size of 215 nm, a polydispersity index of 0.473, and a zeta potential of -26.8 mV, the optimized formulation (F6) had the best entrapment effectiveness of 82.45%, showing nanoscale, stable, and relatively homogeneous vesicles. While DSC thermograms showed the removal of diosgenin's distinctive melting endotherm, confirming the drug's transformation into an amorphous state and effective encapsulation inside the proniosomal matrix, FTIR analysis verified the compatibility of diosgenin with excipients. Sustained drug release was shown by in vitro diffusion experiments, with a cumulative release of 35.06% over a 24-hour period. In comparison to pure diosgenin (9.34 mg/cm<sup>2</sup> flux 0.40 mg/cm<sup>2</sup>/h), ex vivo skin permeation experiments revealed a much increased permeation from the improved formulation (15.30 mg/cm<sup>2</sup> flux 0.66 mg/cm<sup>2</sup>/h). These findings demonstrate that the developed proniosomal cream is a potential transdermal cosmeceutical system and significantly enhances the penetration and distribution of diosgenin.

### ©2025 The authors

This is an Open Access article distributed under the terms of the Creative Commons Attribution (CC BY NC), which permits unrestricted use, distribution, and reproduction in any medium, as long as the original authors and source are cited. No permission is required from the authors or the publishers. (<https://creativecommons.org/licenses/by-nc/4.0/>)

### 1. INTRODUCTION:

As a vital contact between the internal physiological milieu and the exterior world, the skin is the biggest and most versatile organ in the human body<sup>1</sup>. It makes up around 10% of the body's total mass and serves vital functions like thermoregulation, homeostasis maintenance, protection against physical, chemical, and microbiological assaults, and prevention of transepidermal water loss. The skin is crucial in regulating the penetration, distribution, and therapeutic efficacy of topically applied pharmaceutical and cosmeceutical formulations because of its intricate, multilayered structure. The epidermis, dermis, and subcutaneous tissue are the three main layers that make up the skin<sup>2</sup>. Because of its highly organized lipid-protein matrix, the

epidermis—especially the stratum corneum—represents the principal permeability barrier and is the primary rate-limiting step for percutaneous medication absorption. The subcutaneous tissue provides mechanical cushioning, thermal insulation, and serves as a depot for lipophilic substances<sup>3</sup>. While this structural association is vital for physiological protection, it significantly restricts the dermal delivery of many therapeutic agents, particularly phytoconstituents with poor solubility and limited permeability. Topical and transdermal drug delivery systems can avoid first-pass metabolism, maintain sustained drug levels, lessen systemic side effects, and improve patient compliance, they have become viable alternatives to traditional oral and parenteral routes. However, sophisticated carrier-based delivery methods are required due to the stratum corneum's barrier qualities<sup>4</sup>. To improve skin penetration and regulated drug release, vesicular drug delivery methods such as liposomes, niosomes, transfersomes, and ethosomes have been investigated<sup>5</sup>. Proniosomes stand out among these as a particularly promising system because of its exceptional stability, scalability, and ease of handling.

Proniosomes are dry, surfactant-coated carriers that rapidly hydrate upon contact with aqueous media or skin moisture to form niosomal vesicles<sup>6</sup>. Compared to conventional vesicular systems, proniosomes exhibit improved physical and chemical stability, reduced problems of vesicle aggregation, fusion, and drug leakage, and are cost-effective for large-scale manufacturing. Both hydrophilic and lipophilic medications can be effectively encapsulated in their bilayer structure, which is made of cholesterol and non-ionic surfactants<sup>7</sup>. Upon topical application, proniosomes interact with stratum corneum lipids, enhancing drug partitioning, increasing skin permeability, and acting as localized reservoirs for sustained and controlled drug release within the epidermal and dermal layers.

In parallel, there has been a growing demand for cosmeceuticals that integrate cosmetic appeal with therapeutic benefits<sup>8</sup>. These products commonly incorporate natural bioactive compounds that exhibit antioxidant, anti-aging, anti-inflammatory, skin-brightening, and photoprotective properties. Phytoconstituents, in spite of their favourable safety profiles and broad biological activities, often suffer from limitations such as poor aqueous solubility, instability, rapid metabolism, and low bioavailability, which restrict their effectiveness in topical formulations<sup>9</sup>. Nanovesicular delivery systems, particularly proniosomes, provide an effective platform to overcome these challenges by

improving dermal penetration, enhancing stability, and enabling controlled delivery of plant-derived actives.

Due to its numerous pharmacological and cosmetic properties, diosgenin, a naturally occurring steroidal saponin derived from plants like *Trigonella foenum-graecum*, *Smilax* species, and *Dioscorea* spp., has garnered a lot of attention<sup>10</sup>. It displays strong. It is a potential option for dermatological and cosmetic applications because to its antioxidant, anti-inflammatory, anti-aging, tyrosinase-inhibitory, and skin-protective properties<sup>11</sup>.

However, diosgenin's low skin permeability and poor aqueous solubility limit its clinical and topical value, requiring the creation of sophisticated delivery methods to improve its bioavailability and therapeutic efficacy<sup>10</sup>.

These bioactives not only provide complementary cosmeceutical benefits but may also enhance skin interaction and permeability, thereby supporting improved delivery of encapsulated drugs. The incorporation of diosgenin with proniosomes aligns with current trends toward plant-based, multifunctional, and consumer-friendly cosmeceutical products. In light of this, the current work attempts to create and assess a novel proniosomal diosgenin formulation as a cutting-edge topical cosmeceutical delivery method. The work focuses on the formulation and optimization of diosgenin-loaded proniosomes, evaluation of physicochemical characteristics, stability, and dermal delivery performance. By integrating vesicular nanotechnology with natural phytoconstituents, this approach seeks to enhance skin penetration, improve drug retention, and provide sustained therapeutic and cosmetic benefits. The study thus contributes to emerging trends in topical drug delivery by bridging traditional herbal actives with modern proniosomal technology for improved skin therapy.

## 2. MATERIALS AND METHODS:

### Materials:

Span 60 and cholesterol were purchased from Loba Chemie Pvt. Ltd., Mumbai, India. Absolute ethanol and methanol were procured from Fine Chemical Co. Ltd. Diosgenin was kindly provided as a gift sample by Plants Genic Pvt. Ltd., Mumbai, India. All chemicals and reagents employed in this study were of analytical grade and were used without further purification.

### Methods:

#### Formulation of Diosgenin-Loaded Proniosomes: Coacervation Phase Separation Method

Diosgenin-loaded proniosomes were formulated by the coacervation phase separation technique. Precisely weighed amounts of Span 60, cholesterol, and diosgenin were placed in a clean, dry wide-mouth glass vial. A predetermined volume of ethanol was added to serve as the solvent phase, and the vial was tightly closed to avoid solvent loss<sup>12</sup>.

The mixture was heated on a water bath maintained at  $65 \pm 2$  °C for approximately 10 minutes to ensure complete dissolution of the surfactant, cholesterol, and drug, resulting in a clear solution. The formulation was then allowed to cool to room temperature, after which the aqueous phase (phosphate buffer saline) was gradually added,

followed by reheating for an additional 5 minutes to ensure homogeneity. The formulation was then allowed to cool at ambient temperature, resulting in the formation of a proniosomal formulation. The prepared formulation was stored in the same container under dark conditions until further characterization.

#### Composition of Proniosomal Formulations:

Multiple proniosomal formulations (F1–F7) were developed by varying the concentrations of Span 60 and cholesterol while maintaining a constant diosgenin content. Ethanol and phosphate buffer saline served as the solvent and aqueous phases, respectively, to facilitate vesicle formation and stabilization.

**Table 1. Composition of diosgenin-loaded proniosomal formulations.**

Sr.no	Formulation code	Span60 (mg)	Cholesterol (mg)	Drug (mg)	Ethanol (ml)	Phosphate buffer saline (ml)
1	F1	150	50	50	2	3
2	F2	180	90	50	2	3
3	F3	210	70	50	2	3
4	F4	225	80	50	2	3
5	F5	280	60	50	2	3
6	F6	210	100	50	2	3
7	F7	300	50	50	2	3

#### Characterization of Proniosomes:

##### Physical Evaluation-

The prepared proniosomal formulations were subjected to visual inspection to assess their colour, consistency, homogeneity, and the presence of any phase separation, in order to confirm formulation uniformity and physical stability<sup>13</sup>.

The entrapment efficiency of diosgenin in the proniosomal formulations was evaluated by the centrifugation technique. A precisely weighed quantity of proniosomes (0.1 g) was dispersed in 10 mL of phosphate buffer saline (PBS, pH 7.4) in a glass tube and sonicated for 5 minutes to achieve complete dispersion and formation of niosomal vesicles. The resulting dispersion was subsequently centrifuged at 9000 rpm for 45 minutes to separate the vesicular fraction from the free, untrapped drug.

The supernatant containing the free (untrapped) diosgenin was carefully collected and quantified using a UV-visible spectrophotometer at 272 nm, employing phosphate buffer saline (pH 7.4) as the blank. The percentage entrapment efficiency was calculated using the following equation:

$$\text{Entrapment efficacy} = (\text{Total drug} - \text{Untrapped drug}) / \text{Total drug} \times 100$$

##### Drug Content Determination:

Drug content was determined by dissolving an accurately measured volume of proniosomal formulation in a methanol–PBS mixture (pH 7.4)

followed by sonication to ensure complete drug extraction<sup>14</sup>. The solution was filtered, when required, and the absorbance was measured at 272 nm using a UV-visible spectrophotometer. The drug content was determined with reference to a previously constructed calibration curve and expressed as the percentage drug content.

##### FTIR Compatibility Studies:

FTIR spectroscopy was carried out to evaluate possible interactions between diosgenin and formulation excipients. Fourier transform infrared (FTIR) spectra of pure diosgenin, Span 60, cholesterol, and their physical mixture were obtained using an FTIR spectrophotometer over a scanning range of 4000–400 cm<sup>-1</sup>. The samples were prepared by the potassium bromide (KBr) pellet method. The resulting spectra were examined for the characteristic functional group vibrations of diosgenin. The spectra was compared with those of the physical mixture to identify peak shifts, disappearance, or rise of new bands, which could indicate potential chemical interactions.

##### Particle Size, Polydispersity Index, and Zeta Potential:

An aliquot of proniosomal formulation was diluted with deionized water and sonicated until a clear dispersion was obtained<sup>15</sup>. The dispersion was passed through a 0.22 µm membrane filter and subsequently analyzed by dynamic light scattering (DLS) to determine the mean particle size, polydispersity index (PDI), and zeta potential.

**X-Ray Diffraction (XRD) Analysis:**

X-ray diffraction (XRD) analysis was performed to evaluate the crystalline or amorphous characteristics of pure diosgenin and the optimized proniosomal formulation (F6). Diffraction patterns were obtained using a powder X-ray diffractometer equipped with Cu K $\alpha$  radiation ( $\lambda = 1.540 \text{ \AA}$ ) over a 2 $\theta$  range of 5°–60°. The diffractograms were compared on the basis of peak intensity as a function of diffraction angle.

**Differential Scanning Calorimetry (DSC):**

Differential scanning calorimetry (DSC) was employed to evaluate the thermal characteristics of pure diosgenin, the physical mixture, and the optimized diosgenin-loaded proniosomal formulation (F6). Approximately 5 mg of each sample was accurately weighed, sealed in aluminum pans. The samples were scanned over a temperature range of 30–350 °C at a heating rate of 10 °C/min under a nitrogen atmosphere. An empty aluminium pan served as the reference. The resulting thermograms were examined to identify melting endothermic transitions and any alterations in thermal behavior.

**Scanning Electron Microscopy (SEM):**

The surface morphology and structural features of the proniosomal formulations were analyzed using scanning electron microscopy (SEM). The images were studied to determine vesicle shape, surface texture, and the extent of particle aggregation.

**In-Vitro Drug Diffusion Study:**

The *in-vitro* drug diffusion study was conducted using a Franz diffusion cell equipped with a dialysis membrane. A precisely weighed amount of the proniosomal formulation was placed in the donor compartment. The receptor compartment was filled with 20 mL of phosphate buffer saline (PBS, pH 7.4). The diffusion system was maintained at 37 ± 1 °C with the aid of a circulating water jacket. Continuous stirring at 100 rpm was provided using a Teflon-coated magnetic stirrer<sup>16</sup>.

Samples (1 mL) were withdrawn from the receptor compartment at predetermined time intervals over 24 hours and analyzed spectrophotometrically at 272 nm. Each withdrawn sample was replaced with an equal volume of fresh PBS to maintain sink conditions. Based on entrapment efficiency and drug content, formulation F6 was selected as the optimized formulation and compared with pure diosgenin under identical conditions. The cumulative percentage drug diffusion was plotted against time, and the release data were fitted to various kinetic models to elucidate the mechanism of drug release.

**Ex-Vivo Skin Permeation Study:**

*Ex-vivo* permeation studies were carried out using freshly excised goat skin mounted on a Franz diffusion cell. The skin was thoroughly rinsed with cold Ringer's solution and carefully placed between the donor and receptor compartments, with the epidermal surface oriented toward the donor chamber. The proniosomal formulation was uniformly applied to the skin surface, and the exposed area was covered with paraffin paper to minimize dehydration.

The receptor compartment was filled with phosphate buffer saline (PBS, pH 7.4) and maintained at 37 ± 1 °C with continuous stirring at 100 rpm. Aliquots were withdrawn at predetermined time intervals over a 24-hour period and analyzed spectrophotometrically at 272 nm. Each withdrawn sample was replaced with fresh PBS to maintain sink conditions. Optimized formulation F6 was evaluated and compared with pure diosgenin. The cumulative percentage of drug permeated was plotted against time to assess permeation behaviour and mechanism.

**3. RESULTS AND DISCUSSION:**

**Formulation of Diosgenin-Loaded Proniosomes**

Proniosomes of diosgenin were successfully prepared using the coacervation phase separation method. The method is based on the formation of a concentrated surfactant–alcohol system that transforms into a proniosomal formulation upon controlled hydration<sup>17</sup>. This method was selected due to its simplicity, reproducibility, and suitability for producing stable vesicular systems with high drug-loading potential<sup>18</sup>.

To investigate the influence of surfactant concentration on proniosomes formation, formulations were prepared using varying amounts of span 60 (150–300 mg), while the cholesterol concentration was kept constant at 50 mg in all batches. Cholesterol was included to enhance membrane rigidity and stability of the vesicular system. The prepared formulations were visually examined for gel formation, consistency, and appearance.

Among the various formulations evaluated, it was observed that lower concentrations of Span 60 (F1–F5) resulted in semi-solid or less uniform gels. This indicates insufficient surfactant concentration to form a well-organized vesicular structure. In contrast, formulation F6, containing 280 mg of Span 60, produced a smooth, homogeneous proniosomal formulation with a desirable creamy appearance. This suggests that an optimal surfactant-to-cholesterol ratio is critical for effective proniosome formation<sup>19</sup>. At this

concentration, span 60 likely provided adequate bilayer formation and improved encapsulation of diosgenin.

Formulation F7, prepared with a higher span 60 concentration (300 mg), showed a comparatively inferior gel appearance, probably due to excessive surfactant leading to aggregation or reduced structural integrity of the gel system. These observations indicate that increasing surfactant concentration beyond an optimal level does not necessarily improve proniosomal characteristics and may adversely affect gel quality.

Overall, the results demonstrate that the concentration of Span 60 plays a significant role in proniosomes formation and stability<sup>20</sup>. Based on visual appearance and gel-forming ability, formulation F6 was identified as the optimized proniosomal formulation and was selected for further physicochemical characterization and performance evaluation<sup>21</sup>.

#### **Characterization of Proniosomal Formulation: Physical Evaluation-**

All formulations (F1–F7) were visually examined and found to be homogeneous with no phase separation. Formulation F6 exhibited excellent consistency and appearance, indicating optimal surfactant–cholesterol balance and physical stability.

#### **Characterization of prepared proniosomal formulation:**

##### **Physical Assessment:**

Visual evaluation of all prepared diosgenin proniosomal formulations (F1–F7) was carried out to assess colour, consistency, homogeneity, and phase separation. The formulations exhibited colours ranging from brownish semisolid to yellowish white and light yellowish gels, with consistency varying from average to excellent. All batches demonstrated good to excellent consistency and were uniformly homogeneous in appearance. Notably, none of the formulations showed any signs of phase separation, indicating good physical stability. The prepared proniosomal formulation possessed acceptable and desirable physical characteristics, confirming the suitability of the formulation composition and manufacturing process.

##### **Entrapment Efficiency (%):**

The entrapment efficiency (% EE) of the different diosgenin-loaded proniosomal formulations (F1–F7) was evaluated. The % EE ranged from 65.68% (F1) to 82.45% (F6), with the optimized formulation F6 exhibiting the highest entrapment efficiency.

It was observed that formulations with smaller particle sizes demonstrated higher entrapment efficiencies, this indicates an inverse relationship between vesicle size and drug encapsulation. This can be attributed to the fact that smaller vesicles provide a larger surface area-to-volume ratio, allowing more drug to be incorporated into the vesicular bilayers. Among all formulations, F6, which had an optimal particle size of 215 nm, showed superior drug encapsulation, suggesting that this vesicle size is ideal for achieving maximum loading while maintaining stability. The high entrapment efficiency of F6 confirms the successful incorporation of diosgenin into the proniosomal vesicles, supporting its potential for sustained and effective delivery.

##### **FTIR Compatibility Studies:**

Fourier Transform Infrared (FTIR) spectroscopy was employed to investigate the compatibility between diosgenin and the selected excipients, namely span 60 and cholesterol, and to identify any possible chemical interactions during formulation. The FTIR spectrum of pure diosgenin (Fig.1) exhibited characteristic absorption bands corresponding to its functional groups. Prominent peaks were observed at approximately 2897 cm<sup>-1</sup>, attributed to CH<sub>2</sub> stretching vibrations, 1360 cm<sup>-1</sup> corresponding to CH<sub>2</sub> scissoring, and 848 cm<sup>-1</sup> associated with CH<sub>2</sub> twisting vibrations. In addition, a distinct absorption band at 1024 cm<sup>-1</sup> was assigned to C–O stretching, confirming the chemical identity and purity of diosgenin.

The FTIR spectrum of span 60 (Fig. 1) displayed its characteristic peaks, that confirms the presence of ester and aliphatic functional groups typical of non-ionic surfactants. Similarly, cholesterol exhibited its characteristic absorption bands, indicating its structural integrity.

The FTIR spectrum of the physical mixture containing diosgenin, span 60, and cholesterol showed the presence of all major characteristic peaks corresponding to diosgenin without any significant shift in peak position, disappearance, or formation of new peaks. The CH<sub>2</sub> stretching, twisting, and scissoring vibrations observed in pure diosgenin were retained in the physical mixture, and the C–O stretching band at 1024 cm<sup>-1</sup> was also preserved. The retention of these characteristic peaks suggests that diosgenin remained chemically stable and intact in the presence of span 60 and cholesterol.

The absence of prominent changes in the FTIR spectra of the physical mixture indicates that no chemical interaction occurred between diosgenin and the excipients during formulation. These

# Journal of Molecular Science

findings confirm the compatibility of diosgenin with span 60 and cholesterol, supporting their suitability for the preparation of proniosomal formulations. The FTIR results thus demonstrate that the drug-excipient combination is stable and appropriate for further development of diosgenin-loaded proniosomal systems.

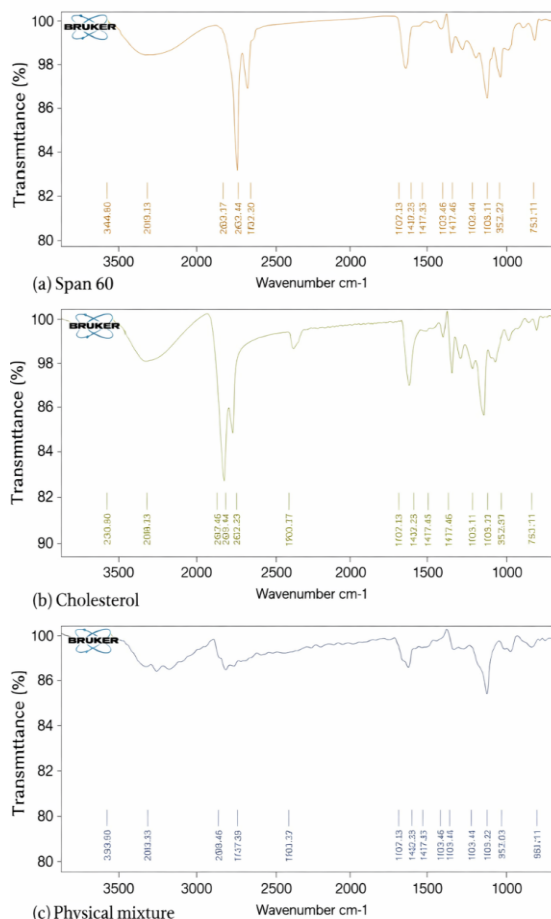


**Figure 1.** FT-IR spectra of pure diosgenin, cholesterol, Span 60 and optimized diosgenin-loaded proniosomal formulation.

## Particle Size, PDI, and Zeta Potential:

The particle size, polydispersity index (PDI), and zeta potential are critical parameters for evaluating the quality, stability, and performance of proniosomal formulations. For the optimized diosgenin-loaded proniosomal formulation (F6), the mean particle size was found to be 215 nm, while the overall mean particle size for the batch was 241 nm. The nanoscale size of the vesicles is advantageous for transdermal delivery, as smaller vesicles can more easily penetrate the stratum corneum, minimize skin irritation, and enhance drug bioavailability at the target site<sup>22</sup>.

The polydispersity index (PDI) of F6 was determined to be 0.473, indicating a moderately homogeneous size distribution of vesicles. A PDI value below 0.5 reflects an acceptable level of

uniformity, which is essential for predictable drug release and reproducible performance of the proniosomal system<sup>21</sup>.

The zeta potential of the optimized formulation was measured as -26.8 mV, suggesting that the vesicles possess sufficient surface charge to maintain colloidal stability. This negative charge generates electrostatic repulsion between vesicles, thereby preventing aggregation or fusion over time and ensures long-term stability of the formulation<sup>23</sup>.

The particle size, PDI, and zeta potential results confirm that the F6 proniosomal formulation exhibits nanosized, stable, and relatively uniform vesicles, making it suitable for efficient transdermal delivery of diosgenin in cosmeceutical applications

## X-ray Diffraction Analysis:

The XRD patterns of the samples (Fig. 2) show differences in crystallinity. The first sample exhibits a broad hump at ~19° 2θ with some sharp peaks, indicating a predominantly amorphous structure with small crystalline domains. The second sample shows multiple sharp peaks with higher intensity, suggesting a more crystalline nature.

The changes in peak intensity and pattern between the two samples indicate structural modification due to formulation or processing. Similar changes were observed in proniosome formulation, where crystallinity is partially reduced in the first sample. These structural changes can enhance solubility, stability, or controlled release, confirming successful formulation of the proniosomes.

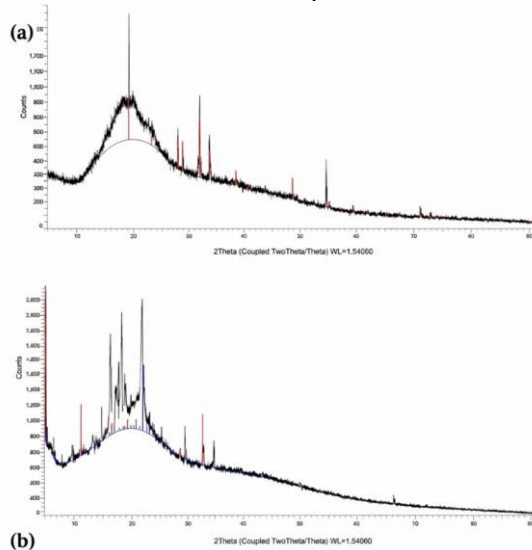


**Figure 2.** X-ray diffraction patterns of diosgenin and optimized diosgenin-loaded proniosomes

## Differential Scanning Calorimetry (DSC):

The DSC thermogram (Fig. 3) of the physical mixture showed distinct endothermic peaks corresponding to diosgenin (280–300 °C),

cholesterol (145–150 °C) and span 60 (50–60 °C), indicating that all components retained their individual crystalline characteristics without any significant interaction.

In contrary, the thermogram of diosgenin proniosomes exhibited complete disappearance of the characteristic melting peak of diosgenin along with marked broadening and shifting of the excipient peaks. The loss of diosgenin's sharp endotherm confirms transformation of the drug from a crystalline to an amorphous or molecularly dispersed state within the proniosomal matrix. The altered thermal behaviour of cholesterol and span 60 further suggests interruption of their crystalline lattices due to strong drug–excipient interactions<sup>24</sup>.

These results confirm successful encapsulation of diosgenin in proniosomes and formation of a stable vesicular system, which is expected to improve the solubility and dissolution properties of diosgenin.

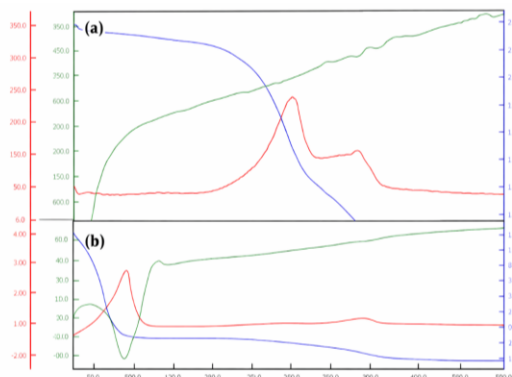


Figure 3. DSC thermograms of (a) physical mixture of diosgenin, cholesterol and Span 60, and (b) diosgenin-loaded proniosomes.

#### Scanning Electron Microscopy (SEM) of Proniosomal Formulation:

Fig.4, shows SEM images of the optimized diosgenin-loaded proniosomal formulation (F6). The SEM micrographs (a–c) represent the surface morphology of the same sample observed at different magnifications. At lower magnification (a), the surface appears relatively uniform with a continuous fibrous network, indicating good structural integrity of the matrix. On increasing the magnification (b), the fibrous nature becomes more evident, with localized thickened regions that suggest partial aggregation or fusion of the material. At the highest magnification (c), the surface shows a rough and irregular texture with the presence of cracks and fragmented regions, which reveals the detailed microstructural features of the sample. Overall, these images confirm that the sample possesses a fibrous and interconnected surface architecture, with minor surface irregularities becoming prominent at higher

magnification.

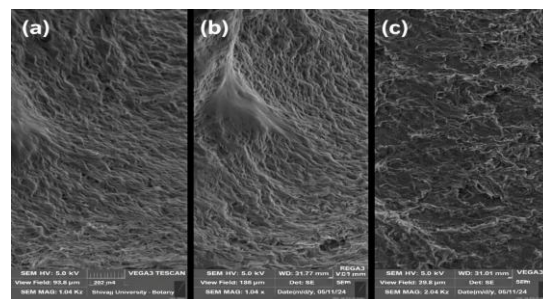


Figure 4. SEM images of optimized diosgenin loaded proniosomes

#### In-Vitro Drug Diffusion and Ex-Vivo Permeability:

The *in-vitro* drug diffusion study of the optimized proniosomal formulation (F6) was performed using goat skin as a model membrane to simulate transdermal drug delivery. The cumulative drug release profile demonstrated a controlled and sustained release of diosgenin from the proniosomal system over a 24-hour period (Fig. 5). Initially, a small amount of unentrapped drug was released rapidly, but most of the drug, encapsulated within the proniosomes, exhibited a gradual and sustained release pattern. The cumulative drug release from F6 reached 35.06 % after 24 hours, whereas the pure diosgenin demonstrated significantly lower release, highlighting the efficiency of proniosomal encapsulation in modulating drug release.

The sustained release observed in F6 is attributed to the presence of cholesterol, which enhances membrane rigidity, stabilizes the vesicular structure, and prevents premature leakage of the drug<sup>25</sup>. The release kinetics of F6 were evaluated using different models, and the Higuchi model showed the highest correlation ( $R^2 = 0.9716$ ), indicating that drug release occurred primarily via diffusion through the vesicular matrix. The Korsmeyer-Peppas model also supported this mechanism ( $R^2 = 0.9633$ ), classifying the release as super case II transport, characteristic of a diffusion-controlled system.

*Ex-vivo* permeability studies further confirmed the improved skin permeation potential of the proniosomal formulation (Fig.6). Using goat skin mounted on a Franz diffusion cell, the optimized formulation (F6) exhibited a cumulative permeation of 15.30 mg/cm<sup>2</sup>, a flux of 0.66 mg/cm<sup>2</sup>/h, and a permeability coefficient of 0.033 cm/h, all of which were markedly higher than the pure diosgenin (9.34 mg/cm<sup>2</sup> cumulative permeation, 0.40 mg/cm<sup>2</sup>/h flux, and 0.02 cm/h permeability). This enhanced permeation is a direct consequence of the nanosized vesicles facilitating

drug penetration through the stratum corneum<sup>26</sup>.

Overall, the *in-vitro* and *ex-vivo* studies demonstrate that the diosgenin-loaded proniosomal formulation (F6) not only provides sustained release but also significantly enhances skin permeation compared to the pure drug, validating its potential as an effective transdermal cosmeceutical delivery system.

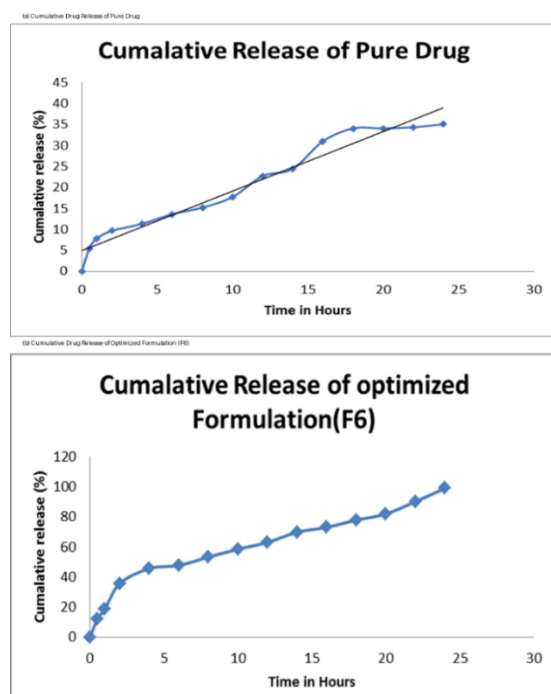
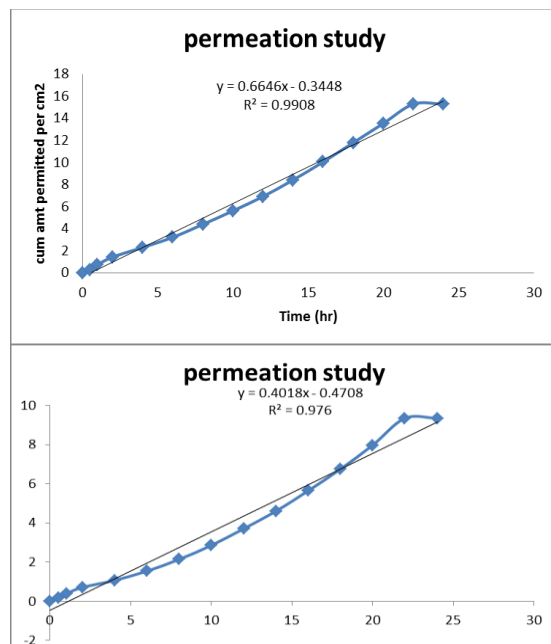


Figure 5. *In-vitro* drug release profile of diosgenin loaded proniosomes and pure drug.



(a) (b)  
 Figure 6. Permeation of drug form optimized formulation(F6) (a) and pure drug (b)

## CONCLUSION:

Diosgenin-loaded proniosomes were successfully formulated using the coacervation phase separation technique and optimized for topical delivery. FTIR studies confirmed the absence of chemical interactions between diosgenin and excipients, indicating good compatibility. DSC analysis revealed the disappearance of the characteristic melting peak of diosgenin in the proniosomal formulation, confirming its transformation from crystalline to amorphous state and successful encapsulation within the vesicular matrix. These findings demonstrate that proniosomal formulation effectively modifies the physicochemical properties of diosgenin, which is expected to enhance its solubility, stability, and skin permeation. Therefore, the developed proniosomal system represents a promising and efficient transdermal cosmeceutical delivery platform for diosgenin.

## REFERENCES

- McKnight J, Shah R, Hargett R. Physiology of the skin. *Surgery (Oxford)*. 2022;40(1):8–12. doi:10.1016/j.mpsur.2021.11.005.
- Menon GK. Skin basics: structure and function. In: *Lipids and Skin Health*. Cham: Springer International Publishing; 2014. p. 9–23.
- Kinnunen HM, Mrsny RJ. Improving the outcomes of biopharmaceutical delivery via the subcutaneous route by understanding the chemical, physical and physiological properties of the subcutaneous injection site. *J Control Release*. 2014;182:22–32.
- Khan MS, Mohapatra S, Gupta V, Ali A, Naseef PP, Kurunian MS, Iqbal Z. Potential of lipid-based nanocarriers against two major barriers to drug delivery—skin and blood–brain barrier. *Membranes*. 2023;13(3):343.
- Witika BA, Mweetwa LL, Tshiamo KO, Edler K, Matafwali SK, Ntemi PV, Makoni PA. Vesicular drug delivery for the treatment of topical disorders: current and future perspectives. *J Pharm Pharmacol*. 2021;73(11):1427–1441.
- Reddy KTK, Gandla K. Novel vesicular drug delivery systems: proniosomes. *Pharm Res*. 2022;6(3):000272.
- Ruwizhi N, Aderibigbe BA. The efficacy of cholesterol-based carriers in drug delivery. *Molecules*. 2020;25(18):4330.
- Shastri DH, Gandhi S, Almeida H. Enhancing collaboration and interdisciplinary strategies for navigating innovative technologies and regulatory approvals in the cosmetic industry. *Curr Cosmet Sci*. 2024.
- Mouhid L, Corzo-Martínez M, Torres C, Vázquez L, Reglero G, Fornari T, Ramírez de Molina A. Improving *in vivo* efficacy of bioactive molecules: an overview of potentially antitumor phytochemicals and currently available lipid-based delivery systems. *J Oncol*. 2017;2017:7351976.
- Sewal P, Painuli S, Abu-Izneid T, Rauf A, Sharma A, Daştan SD, Cho WC. Diosgenin: an updated pharmacological review and therapeutic perspectives. *Oxid Med Cell Longev*. 2022;2022:1035441.
- Lee J, Jung K, Kim YS, Park D. Diosgenin inhibits melanogenesis through the activation of phosphatidylinositol-3-kinase pathway signaling. *Life Sci*. 2007;81(3):249–254.
- Mokale VJ, Patil HI, Patil AP, Shirude PR, Naik JB. Formulation and optimisation of famotidine proniosomes: an *in vitro* and *ex vivo* study. *J Exp Nanosci*. 2016;11(2):97–110.
- Patil HI, Patil AA, Patil DD, Wadkar KA, Vanjari AV.

Formulation and development of *Carica papaya* leaf extract loaded proniosomes: dose reduction and enhanced absorption. *Int J Biol Med Res.* 2025;16(2):8019–8022.

- 14. Nimbalwar M, Upadhye K, Dixit G. Fabrication and evaluation of ritonavir proniosomal transdermal gel as a vesicular drug delivery system. *Pharmacophore.* 2016;7(2–2016):82–95.
- 15. Gaja JB, Selvam PR. Proniosomes: a review on provesicular drug delivery system. *EJPPS.* 2025;301. doi:10.37521/ejpps30101.
- 16. Abdelbary GA, Amin MM, Zakaria MY. Ocular ketoconazole-loaded proniosomal gels: formulation, ex vivo corneal permeation and in vivo studies. *Drug Deliv.* 2017;24(1):309–319.
- 17. Vora B, Khopade AJ, Jain NK. Proniosome based transdermal delivery of levonorgestrel for effective contraception. *J Control Release.* 1998;54(2):149–165.
- 18. Bayindir SZ, Yuksel N. Provesicles as novel drug delivery systems. *Curr Pharm Biotechnol.* 2015;16(4):344–364.
- 19. Kulkarni P, Shirasand SB, Mutalik S, Hiraskar A, Pokale R, Mukharya A. Impact of cholesterol and surfactant selection on tacrolimus-loaded niosomes for transdermal drug delivery. *Micro Nanosyst.* 2025;[volume and page numbers pending].
- 20. Nadzir MM, Fen TW, Mohamed AR, Hisham SF. Size and stability of curcumin niosomes from combinations of Tween 80 and Span 80. *Sains Malaysiana.* 2017;46(12):2455–2460.
- 21. Mujtaba MA, Kaleem M, Chaware R, Ingole A, Asiri YI, Hassan MZ, Aldawsari MF. Development and optimization of proniosomal formulation of irbesartan using a Box–Behnken design to enhance oral bioavailability: physicochemical characterization and in vivo assessment. *ACS Omega.* 2024;9(14):16346–16357.
- 22. Matharoo N, Mohd H, Michniak-Kohn B. Transferosomes as a transdermal drug delivery system: dermal kinetics and recent developments. *Wiley Interdiscip Rev Nanomed Nanobiotechnol.* 2024;16(1):e1918.
- 23. Bautista-Solano AA, Dávila-Ortiz G, Perea-Flores MDJ, Martínez-Ayala AL. A comprehensive review of niosomes: composition, structure, formation, characterization, and applications in bioactive molecule delivery systems. *Molecules.* 2025;30(17):3467.
- 24. de Vos L, Gerber M, Liebenberg W, Wessels JC, Lemmer HJ. Co-processed crystalline solids of ivermectin with Span® 60 as solubility enhancers of ivermectin in natural oils. *AAPS PharmSciTech.* 2024;25(4):67.
- 25. Ali MA, Mohamed MI, Megahed MA, Abdelghany TM, El-Say KM. Cholesterol-based nanovesicles enhance the in vitro cytotoxicity, ex vivo intestinal absorption, and in vivo bioavailability of flutamide. *Pharmaceutics.* 2021;13(11):1741.
- 26. Yu YQ, Yang X, Wu XF, Fan YB. Enhancing permeation of drug molecules across the skin via delivery in nanocarriers: novel strategies for effective transdermal applications. *Front Bioeng Biotechnol.* 2021;9:646554.